Transition from smooth sliding to stick-slip motion in a single frictional contact

O. M. Braun*
Institute of Physics, National Academy of Sciences of Ukraine, 03028 Kiev, Ukraine

M. Peyrard
Laboratoire de Physique de l'Ecole Normale Supérieure de Lyon, 46 Allée d'Italie, 69364 Lyon Cédex 07, France

V. Bortolani, A. Franchini, and A. Vanossi
INFM-S3 e Dipartimento di Fisica, Universitá di Modena e Reggio Emilia, Via Campi 213/A, 41100 Modena, Italy
(Received 14 June 2005; published 14 November 2005)

We show that the transition from smooth sliding to stick-slip motion in a single planar frictional junction always takes place at an atomic-scale relative velocity of the substrates.

DOI: 10.1103/PhysRevE.72.056116 PACS number(s): 81.40.Pq, 46.55.+d

I. INTRODUCTION

The problem of friction between two substrates which are in moving contact is very rich physically as well as very important technologically [1–5]. Following the development of atomic force microscopy, studying tribology has approached the microscopic level, while nanotechnology begins to build devices so miniaturized that they probe the microscopic properties of the materials. This explains the interest of numerical simulations of the friction [5–16].

When the static frictional force is nonzero, the friction generally displays two different regimes: a stick-slip motion at low driving velocities and smooth sliding at high velocities. In most cases the stick-slip regime is not desired and has to be avoided. This requires the knowledge of the mechanisms of these two regimes and an understanding of the transitions between them.

The question of interest of the present work is *the microscopic mechanism of the transition from smooth sliding to stick-slip motion*. In a previous work [16], we studied the motion of two substrates separated by a thin lubricant film at small velocity of the top substrate v_{top}, looking for the smallest possible value of the velocity for which the motion stays smooth. We have shown that *the microscopic transition from sliding to stick-slip takes place at a velocity which is many orders of magnitude higher than that observed in macroscopic experiments*. The same result was also obtained in almost all other simulations (e.g., see review papers [5] and references therein). Namely, the experiments typically demonstrate the transition from stick-slip to smooth sliding at a threshold velocity $v_c \sim 1$ μm/s, while the simulations give values $v_c \sim 10$ m/s, which are atomic-scale values because they correspond to moving along a length of the order of a lattice spacing (1 Å) in a time of the order of the period of atomic vibrations (10^{-11} s).

This suggests that the macroscopic mechanism of the transition from stick-slip motion to smooth sliding is completely different from the microscopic one. However, in simulation the system size available for the study is always rather small so that the simulation can describe rigorously neither the elastic properties of the substrates nor the inertia effects due to a macroscopically large mass of the sliding substrate. This leaves room for speculation that the disagreement between the simulations and experimental results is connected with the too small size of the simulated system. This is the point that we want to clarify in the present work. *We shall prove that the transition from smooth sliding to stick-slip motion in a single microscopic frictional junction always takes place at an atomic-scale relative velocity of the substrates*, even if this contact is between a substrate and a very large sliding block, which could even extend to infinity in the direction perpendicular to the sliding plane.

In the simplest model of friction, both substrates are treated as rigid. This reduces the model to one body, a "particle," moving in a periodic potential created by the bottom substrate, in the presence of friction, and driven by an external force. This model allows a rigorous treatment as summarized in the monograph by Risken [17]. At zero temperature, $T=0$, the average velocity $\langle v \rangle$ of the single driven particle as a function of the dc driving force F exhibits hysteresis. To be specific, let us consider a particle of mass M subjected to an external sinusoidal potential $V(x)$ with an amplitude $\mathcal{E}=\max[V(x)]-\min[V(x)]$ and a period a. If the particle is driven by a force F, it starts to move when F exceeds the value $F_s=\pi\mathcal{E}/a$. If the force is then reduced gradually, a backward transition occurs when the force drops below a threshold $F=F_b=(2\sqrt{2}/\pi)\eta\sqrt{M\mathcal{E}}$, where η is the viscous damping coefficient. Thus, in the underdamped case, $\eta<\eta_c\equiv(\pi^2/2\sqrt{2})\sqrt{\mathcal{E}/Ma^2}=(\pi/4)\omega_s$ [where $\omega_s=(2\pi/a)\sqrt{\mathcal{E}/2M}$ is the frequency of small-amplitude oscillation of the particle at the bottom of the external potential], we have $F_b<F_s$, and the system exhibits hysteresis due to the inertia of the particle. In this simplest model of friction, the forward locked-to-running transition corresponds to overcoming the static friction force F_s, while the threshold force F_b is the kinetic frictional force. The inequality $F_b<F_s$ is the necessary condition for existence of stick-slip.

The threshold force F_b can be found from a calculation of energy gain and loss. When the particle moves for the dis-

*Electronic address: obraun@iop.kiev.ua

tance a (one period of the external potential), it gains the energy $E_{\rm gain}=Fa$ from the driving and loses some energy $E_{\rm loss}$ due to friction. In the steady state these energies must be equal to each other: $E_{\rm gain}=E_{\rm loss}$. Thus, the backward threshold force for the transition from the sliding (running) motion to the locked (pinned) state is determined by $F_b=\min(E_{\rm loss})/a$. The energy loss is caused by an external frictional force $F_{\rm fric}(t)=M\eta v(t)$, which models the energy transfers into the substrate. It is given by

$$E_{\rm loss}=\int_0^\tau dt\, F_{\rm fric}(t)v(t)=\int_0^\tau dt\, M\eta v^2(t)=M\eta\int_0^a dx\, v(x), \tag{1}$$

where $\tau=a/\langle v\rangle$ is the "washboard period;" i.e., the time for motion over the distance a at the average velocity $\langle v\rangle$. The minimal loss is achieved when the particle has zero velocity on top of the total external potential: $V_{\rm tot}(x)=V(x)-Fx$.

In the limit $\eta\to 0$ and $F\to 0$, the minimal energy loss can easily be found analytically. From the energy conservation law, $\frac{1}{2}Mv^2+\frac{1}{2}\mathcal{E}[1-\cos(2\pi x/a)]=\mathcal{E}$, we can find the particle velocity $v(x)$. Substituting it into Eq. (1), we obtain

$$F_b=\frac{M\eta}{a}\left(\frac{\mathcal{E}}{M}\right)^{1/2}\int_0^a dx\left[1+\cos\left(\frac{2\pi x}{a}\right)\right]^{1/2}=C\eta(\mathcal{E}M)^{1/2}, \tag{2}$$

where the numerical constant

$$C\equiv(2\pi)^{-1}\int_0^{2\pi}dy(1+\cos y)^{1/2}=2\sqrt{2}/\pi\approx 0.9$$

depends only on the shape of the external potential. Equation (2) can be rewritten as

$$F_b=M\eta\bar{v}=(2/\pi)M\eta v_m,$$

where $\bar{v}=a^{-1}\int_0^a dx\, v(x)$, and $v_m=(2\mathcal{E}/M)^{1/2}=\pi\bar{v}/2$ is the maximum velocity achieved by the particle when it moves at the bottom of the external potential. Note that the average particle velocity, $\langle v\rangle=\tau^{-1}\int_0^\tau dt\, v(t)=a/\tau$, tends continuously to zero when $F\to F_b$, because $\tau\to\infty$ in this limit.

Figure 1 shows the time evolution of the velocity $v(t)$ in a case where the driving force F slowly decreases with time. In this figure and in the remainder of the paper we use a dimensionless system of units, where $a=2\pi$ and $\mathcal{E}=2$.

Although the transition from the sliding motion to the locked state is continuous, the velocity drops quite sharply at the threshold force $F=F_b$ ($F_b\approx 0.127$ for $\eta=0.1$ and $M=1$). When the force changes adiabatically, the hysteresis of the function $v(F)$ only exists for $T=0$. At any small but nonzero temperature, there is no hysteresis for a single particle. The transition from the locked state, which in this case is actually a state in which the particle moves by thermally activated jumps from a potential well to another, to the running state, and the backward sliding-to-locked transition, both take place for the same value of the force $F=C'\eta(\mathcal{E}M)^{1/2}$, where $C'\approx 2.3742$ [17,18]. However, if the force F changes with a finite rate $r=\Delta F/\Delta t>0$, the hysteresis still exists, especially at high rates ($r>F_s\eta$).

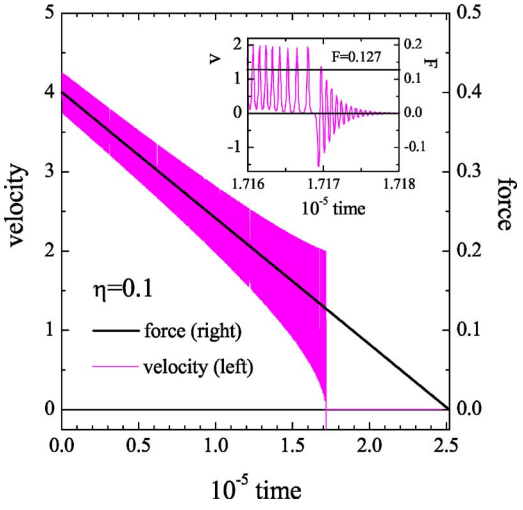

FIG. 1. (Color online) The velocity of the atom (gray curve) versus time when the force (black solid line) smoothly decreases. Inset: zoom of the transition at $F=F_b=0.127$ ($M=1$, $\eta=0.1$).

More complicated models, such as a one-dimensional (1D) chain of interacting atoms in a periodic substrate potential (the Frenkel-Kontorova model) [12,19], a two-dimensional array of atoms in a two-dimensional periodic potential [9,10,19], and even a three-dimensional (3D) model of friction, where two rigid substrates are separated by a thin lubricant film [16] (see Sec. III B) exhibit properties which are qualitatively similar to the simple one-particle model. In all these models, the sliding-to-locked transition takes place at an atomic-scale velocity of the sliding block.

However, the characteristic velocity of the transition depends on the mass of the moving substrate. As shown above, it may be estimated to be $v_m\propto(\mathcal{E}/M)^{1/2}$, where $\mathcal{E}=N_s\varepsilon$, N_s is the number of atoms at the interface, and ε is the barrier per one surface atom. When the sliding block is considered as *rigid*, then $M=N_sN_\perp m$, where m is the atomic mass and $N_\perp$ is the number of atomic layers in the block. Thus, for a macroscopically large block ($N_\perp\to\infty$), the velocity at the transition may be made as small as desired ($v_m\propto N_\perp^{-1/2}$), e.g., as low as the velocities observed experimentally, which might seem to reconcile theory and experiments. This is, however, an oversimplified view that is wrong, as was first mentioned by Persson [11]. The reason is that for a *nonrigid* substrate, only the atomic layer which is the closest to the substrate stops at the transition so that $M=mN_s$, and v_m should be of atomic-scale value. In the present work we prove that for the case of a planar geometry of the sliding contact, this is indeed the case, even if the sliding block has an infinite mass. This is in agreement with recent molecular dynamics (MD) results due to Luan and Robbins [25]. Moreover, we show that when the moving object has its own internal degrees of freedom that can be excited due to sliding (as it is in the case of sliding of the top block in tribology experiments), then the transition becomes discontinuous.

The paper is organized as follows. The study is split into two sections: Sec. II, wherein the case of a dry friction is discussed, and Sec. III, wherein the system with a thin lubricant film is studied. In Sec. II A we present the Green-

function technique, which allows an analytical calculation of the kinetic frictional force for a simple model. This technique is applied in Sec. II B to a simplified one-dimensional model of the top substrate, where most results may be obtained analytically in a closed form. The analytical results are compared with the numerical ones in Sec. II C, which confirms the accuracy of the analytical approach. In this subsection we also show the difficulty of an accurate simulation of the sliding-to-locking transition. The Green-function technique is then applied in Sec. II D to the three-dimensional model of the semi-infinite top substrate, which cannot be studied with MD simulation. In Sec. III the system with two substrates separated by a thin lubricant film is studied. In Sec. III A we first describe a simplified model which demonstrates the layer-over-layer sliding. We then present the results of a realistic 3D simulation of the lubricant system. The model used in simulation is briefly described in Sec. III B. We then consider two typical examples of the lubricant: the case of a "hard" lubricant in Sec. III C, in which the lubricant film remains in a solid state during sliding, and the case of a "soft" lubricant in Sec. III D, in which the lubricant is melted during sliding. In both cases we demonstrate that the velocity of sliding-to-locked transition is of atomic-scale value. The same is true for the critical velocity of the transition from the stick-slip motion to smooth sliding, as discussed in Sec. III E. Finally, Sec. IV concludes the paper with a short discussion.

II. DRY FRICTION

Let us begin with the simplest case of "dry friction," in which the top substrate is in direct contact with the bottom substrate. The case of two substrates separated by a thin lubricant film will be considered in Sec. III.

A. Green-function technique

In general the frictional force acting on the top block when it moves over the periodic external potential created by the bottom substrate, can be found by equating the energy gain and loss. In what follows it will be convenient to split the total kinetic frictional force into three contributions that we shall examine separately:

$$F = F_1 + F_2 + F_3. \tag{3}$$

These forces designate the average of each contribution for the motion of the sliding block over one lattice spacing of the substrate.

The first contribution F_1 in Eq. (3) describes the flow of energy into the top substrate that is due to internal degrees of freedom (phonons) in the moving block. Namely, when the top block moves with an average velocity $\langle v\rangle$, the atoms in the lowest layer of the top block are excited by a force coming from the interaction with the substrate. Its main component is oscillating at the washboard frequency $\omega_0=(2\pi/a)\times\langle v\rangle$. According to the linear response theory [20], when a system is excited by a small periodic force $f(t)=\mathrm{Re}\, f_0 \exp(i\omega_0 t)$ with the frequency ω_0 and amplitude f_0 (here f_0 is real), then its velocity oscillates with the (complex) amplitude

$$v_0 = i\omega_0 x_0, \quad x_0 = \alpha(\omega_0) f_0, \tag{4}$$

where $\alpha(\omega)$ is the generalized susceptibility. The rate of energy loss (i.e., the energy absorbed by the top block per one time unit) is then equal to

$$R = \frac{1}{2} f_0^2 \omega_0 \,\mathrm{Im}\, \alpha(\omega_0). \tag{5}$$

It is convenient to define the (causal) phonon Green function $G(\omega)$ by the equation [21]

$$(\omega^2 - i\omega\eta_l - \mathbf{D}) \quad G(\omega) = 1, \tag{6}$$

where $\mathbf{D}$ is the elastic matrix of the semi-infinite top substrate and η_l is the damping inside the block. In our case we consider the limit $\eta_l \to 0$, but it is not set to be strictly equal to 0 for definiteness of the response function. The susceptibility $\alpha(\omega)$ can then be expressed through the Green function as $\alpha(\omega)=-G(\omega)/m$ (here ω must be real). Actually, for a crystal lattice, the excitation can be applied at any site, so that it is a matrix, as well as the response, and both α and G are tensors. However, for our applications wherein the excitation is restricted to the sliding plane, and we are interested in the response of the atoms in this plane, we can restrict the analysis to some of their scalar components, as discussed below.

The rate of energy loss can now be obtained from

$$R = \frac{\pi}{4} \frac{f_0^2}{m} \rho(\omega_0), \tag{7}$$

where $\rho(\omega)$ is related to the Green function $G(\omega)$ by

$$\rho(\omega) = -\frac{2}{\pi} \omega \,\mathrm{Im}\, G(\omega) \tag{8}$$

is the local density of phonon modes in the top substrate because it is deduced from the component of the tensor G which involve surface atoms. The density $\rho(\omega)$ is normalized to unity, $\int_0^\infty d\omega \rho(\omega)=1$. The energy absorbed by the top substrate during its motion for one period of the external potential is equal to $E_{\mathrm{loss}}^{(1)}=R\tau=2\pi R/\omega_0=Ra/\langle v\rangle$, and the contribution F_1 can be found as $F_1=E_{\mathrm{loss}}^{(1)}/a$, or

$$F_1 = \frac{\pi}{4} \frac{f_0^2}{m\langle v\rangle} \rho(\omega_0). \tag{9}$$

The contributions $F_2+F_3=m\eta\bar{v}$ in Eq. (3) are due to the external damping of the atoms of the lowest layer of moving block that are in contact with the substrate, similar to the scenario described above in Sec. I for the single-particle model. The flux of energy into the bottom substrate is due to the excitation of phonons and to the transfer of electrons above the Fermi level, creating holes below. For simplicity, and because we are interested in qualitative results only, let us assume that the coefficient η is constant (see, however, Sec. III B, wherein the 3D simulations are described). It is

convenient to split the friction force describing this energy transfer to the substrate $a^{-1}\int_0^\tau m\eta v^2(t)dt$ into two parts: the "trivial" contribution

$$F_2 = m\eta\langle v\rangle \tag{10}$$

and the "fluctuating" contribution

$$F_3 = \frac{m\eta}{a}\int_0^\tau dt[v^2(t) - \langle v\rangle^2] = \frac{m\eta}{\langle v\rangle}\frac{1}{\tau}\int_0^\tau dt[v(t) - \langle v\rangle]^2. \tag{11}$$

This fluctuating contribution, which grows at low velocities, finally leads to the transition from the smooth sliding to the locked state.

If we take into account only the lowest harmonic of the washboard frequency,

$$v(t) = \langle v\rangle + |v_0|\cos(\omega_0 t + \phi),$$

then

$$F_3 = \frac{1}{2}\frac{m\eta}{\langle v\rangle}|v_0|^2. \tag{12}$$

The amplitude $|v_0|$ can again be found with the help of the linear response theory, $|v_0| = \omega_0|\alpha(\omega_0)|f_0$ according to Eq. (4), so that the contribution F_3 can be expressed as

$$F_3 = \frac{\eta f_0^2}{2m}\left(\frac{2\pi}{a}\right)^2 |G(\omega_0)|^2\langle v\rangle, \tag{13}$$

where we put $f_0 = F_s$. Note that for the single atom, the threshold force for locking was determined by the F_3 contribution only. However, when the moving block has internal degrees of freedom, then $F_1 > 0$, and the velocity of the running-to-locked transition may be nonzero, so that $F_2 > 0$ as well.

Above we considered only the contribution from the first harmonic of the force exerted by the substrate, which is at the washboard frequency. In the general case, however, we have to expand the trajectory $x(t)$ into a Fourier series and then sum over the contributions of all harmonics $\omega_n = (n+1)\omega_0$, $n = 0, \ldots, \infty$. Numerically, for a given $\langle v\rangle$ we have to start with some approximate shape of $x(t)$ [e.g., $x(t) = \langle v\rangle t$] and then calculate step by step the force acting on the atoms of the top block,

$$f(t) = -\sin x(t) - m\eta\dot{x}(t), \tag{14}$$

make its Fourier transform,

$$f_n = \int_0^\tau dt\, e^{i\omega_n t} f(t), \tag{15}$$

find the velocity in response to this force,

$$v_n = -i\omega_n f_n G(\omega_n), \tag{16}$$

then perform the backward Fourier transform,

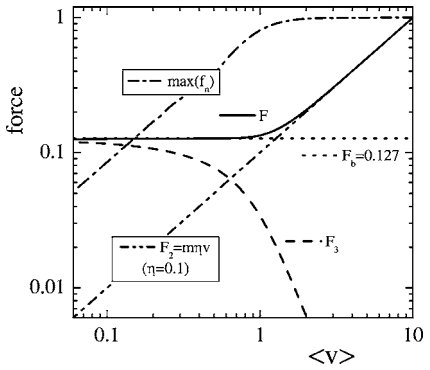

FIG. 2. The total frictional force F and its contributions F_2 and F_3 as functions of the averaged velocity $\langle v\rangle$ for the single atom calculated by the Green-function technique for $\eta = 0.1$ and $m = 1$. We also plot the amplitude of the maximum harmonic $\max|f_n|$, which is equal to 1 when the main washboard harmonics dominates, but begins to decrease when high-order harmonics begin to contribute.

$$v(t) = (2\pi)^{-1}\omega_0\sum_{n=0}^{\infty} e^{-i\omega_n t}v_n, \tag{17}$$

and finally calculate $x(t)$ as the integral of $v(t)$ over time; the output trajectory must coincide with the input one. Repeating these operations iteratively, one can find the self-consistent trajectory. Then, the radiation contribution has to be calculated as

$$F_1 = -\frac{1}{2m\langle v\rangle}\sum_{n=0}^{\infty}\omega_n|f_n|^2\,\mathrm{Im}\,G(\omega_n)$$

$$= -\frac{\pi}{am}\sum_{n=0}^{\infty}(n+1)|f_n|^2\,\mathrm{Im}\,G(\omega_n), \tag{18}$$

the trivial contribution is given by Eq. (10), and the fluctuating contribution by Eq. (11), or

$$F_3 = \frac{m\eta}{2\langle v\rangle}\sum_{n=0}^{\infty}|v_n|^2 = \frac{\eta\langle v\rangle}{2m}\left(\frac{2\pi}{a}\right)^2\sum_{n=0}^{\infty}(n+1)^2|f_n G(\omega_n)|^2. \tag{19}$$

Applying this procedure for the case of a single atom, when $G(\omega) = \omega^{-2}$, we obtain the dependencies shown in Fig. 2 (of course, for the single atom these dependencies can easily be calculated directly by integrating the motion equation; we used this fact to test the accuracy of the Green-function technique). One can see that the harmonics with $n \geqslant 1$ begin to be important at low velocities $\langle v\rangle < 1$ only. We also see that the total frictional force F decreases monotonically with decreasing of $\langle v\rangle$, and the sliding-to-locked transition is continuous; i.e., $\langle v\rangle \to 0$ when $F \to F_b$. However, below we show that already for a simple one-dimensional model of the top sliding substrate, the transition becomes discontinuous.

B. One-dimensional semi-infinite substrate: analytics

Let us first apply the Green-function technique to a simplified model when the top substrate is modeled by the semi-

infinite one-dimensional chain of atoms oriented perpendicularly to the bottom substrate. In this case most of the results can be obtained analytically. Namely, if the atoms are coupled by harmonic springs with the elastic constant g and the lattice constant a_s, then the chain is characterized by the phonon spectrum

$$\omega^2(k) = 2g(\cos ka_s - 1),$$

or $\omega(k)=\omega_m \sin(a_s k/2)$, where $\omega_m=2\sqrt{g/m}$ is the maximum phonon frequency of the top block. The Green function for the semi-infinite one-dimensional chain can be found by the standard technique [21,22]. For this one-dimensional model the Green function is actually a matrix. However, as the excitation is applied to site 1 in the lattice, and we are interested in the response of this site 1, we only need its component $G_{11}(\omega)$, which we shall denote by the simplified notation $G(\omega)$. The calculation yields

$$\mathrm{Im}\, G(\omega) = -\frac{2}{\omega_m^2}\left(\frac{\omega_m^2}{\omega^2} - 1\right)^{1/2} \tag{20}$$

inside the phonon zone ($|\omega|<\omega_m$), and $\mathrm{Im}\, G(\omega)=0$ outside the zone ($|\omega|\geqslant\omega_m$). The real part of the Green function is constant inside the zone [$\mathrm{Re}\, G(\omega)=2/\omega_m^2$ for $|\omega|\leqslant\omega_m$], while outside the zone ($|\omega|>\omega_m$), the real part is equal to

$$\mathrm{Re}\, G(\omega) = \frac{2}{\omega_m^2}\left[1 - \left(\frac{x-1}{x+1}\right)^{1/2}\right], \tag{21}$$

where $x=2\omega^2/\omega_m^2-1$. The surface phonon density of states $\rho_{11}(\omega)$ [denoted by the simplified notation $\rho(\omega)$] is related to $G_{11}=G(\omega)$ by Eq. (8). It is equal to

$$\rho(\omega) = \frac{4}{\pi\omega_m}\left(1 - \frac{\omega^2}{\omega_m^2}\right)^{1/2}, \quad |\omega| \leqslant \omega_m. \tag{22}$$

The substitution of this expression into Eq. (9) yields

$$F_1 = \frac{1}{4}\left(\frac{2\pi}{a}\right)\frac{f_0^2}{g}\left[\left(\frac{a}{2\pi}\right)^2 \frac{4g}{m\langle v\rangle^2} - 1\right]^{1/2}, \tag{23}$$

provided the washboard frequency is inside the phonon spectrum ($\omega_0<\omega_m$). In the low-velocity limit ($\langle v\rangle\to 0$), Eq. (23) leads to

$$F_1 \approx \frac{1}{2}\frac{f_0^2}{\sqrt{mg}}\frac{1}{\langle v\rangle}. \tag{24}$$

Thus, the phonon contribution to the frictional force tends to infinity at low velocities because the density of phonon states (22) is nonzero at $\omega=0$ for one-dimensional systems (for the three-dimensional model of the substrate, the situation is more delicate, see Sec. II D).

From Eqs. (4) and (20) we have $|v_0|=2f_0/m\omega_m$ and

$$|G(\omega_0)|^2 = \frac{4}{\omega_m^2\omega_0^2} = \frac{4}{\omega_m^2}\left(\frac{a}{2\pi}\right)^2 \frac{1}{\langle v\rangle^2}, \tag{25}$$

so that the contribution F_3 is equal to

$$F_3 = \frac{\eta f_0^2}{2g\langle v\rangle}. \tag{26}$$

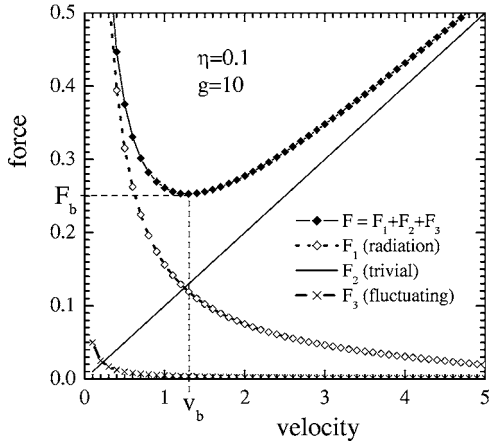

FIG. 3. The frictional force (solid curve and solid diamonds) as a function of the velocity for the one-dimensional model of the top substrate with $m=1$, $g=10$ ($\omega_m\approx 6.32$) and $\eta=0.1$, and the contribution F_1 [Eq. (23)] due to radiation into the top substrate (dotted curve and open diamonds), the trivial contribution $F_2=m\eta\langle v\rangle$ (solid line), and the fluctuating contribution F_3 [Eq. (26)] (dashed curve and crosses). The solution to the right of the minimum, $v\geqslant v_b$ corresponds to the stable motion, while the solution in the $v<v_b$ interval corresponds to the unstable motion.

The function $F(v)$ is shown in Fig. 3, together with the contributions $F_1(v)$, $F_2(v)$, and $F_3(v)$.

The function $F(v)$ has a minimum at $v=v_b\approx 1.3$, where $F(v_b)=F_b\approx 0.253$. The part of the $F(v)$ curve to the right of the minimum ($v\geqslant v_b$) corresponds to the stable motion, while the solution for $v<v_b$ interval is unstable. Therefore, when the velocity decreases below v_b, the system must switch abruptly to the locked state. This is an important result of the present work: if the dc force applied to the upper layer of the top substrate gradually decreases, then the transition from the sliding regime to the locked state that occurs at $F=F_b$ takes place when the average velocity of the top block is nonzero ($v_b>0$), contrary to the scenario of the single-particle model described in Sec. I. The dependencies F_b and v_b on the external damping η are shown in Fig. 4.

For not too small external damping, when $v_b<(a/2\pi)\omega_m$, one can find approximately that

$$v_b \approx \frac{f_0}{(4m^3g)^{1/4}}\frac{1}{\sqrt{\eta}} \tag{27}$$

and

$$F_b \approx f_0(4m/g)^{1/4}\sqrt{\eta}. \tag{28}$$

We emphasize that the threshold values do not depend on the size of the top block or on its total mass, although they depend on its elasticity, a larger g leading to lower values for both thresholds. However, these dependencies are weak; F_b and $v_b \propto g^{-1/4}$ only.

The analytical results presented above were obtained for the case in which only the main harmonic of the washboard frequency was taken into account. However, from the full

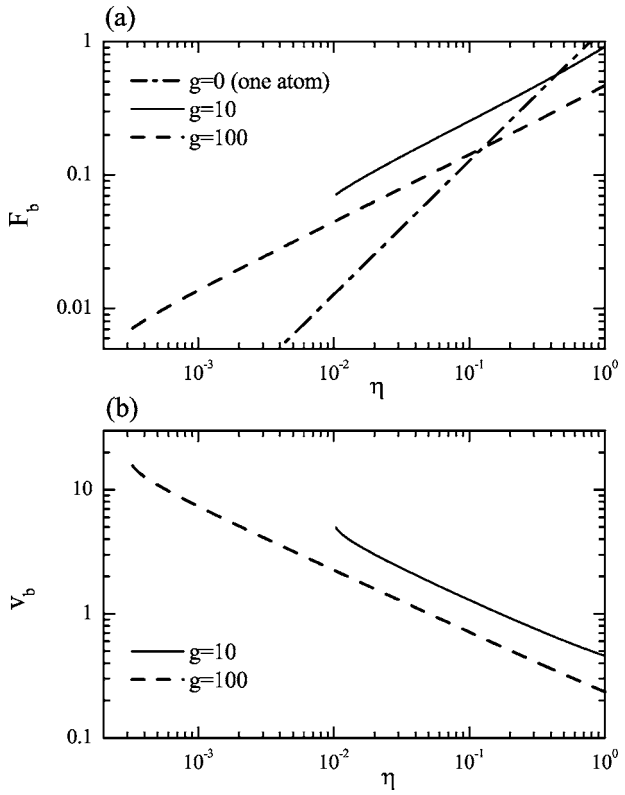

FIG. 4. (a) The threshold force F_b and (b) the velocity v_b for the sliding-to-locked transition as functions of the external damping η in the 1D model of the top substrate for two values of the substrate elastic constant $g=10$ ($\omega_m \approx 6.32$, solid curves) and $g=100$ ($\omega_m = 20$, dashed curves); $m=1$.

self-consistent calculation, we found that the contribution of higher harmonics becomes important only at $v \ll 1$, as shown in Fig. 5.

It should be noticed that the minimum of $F(v)$ for $v=v_b$ is related to the rise of F_1 for low velocity, i.e., a sharp increase

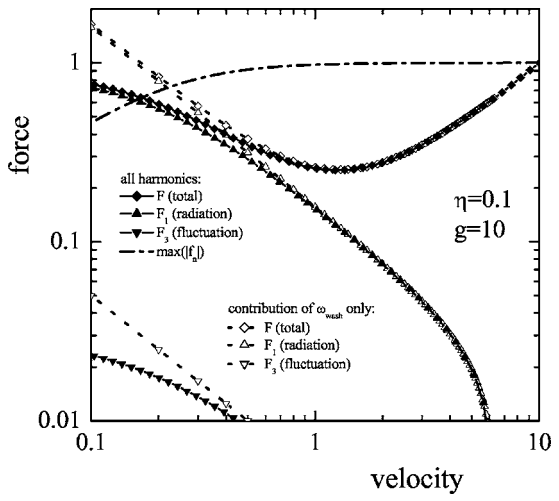

FIG. 5. The comparison of the self-consistent calculation (solid curves and solid symbols) and those with the main harmonics of the washboard frequency only (dotted curves and open symbols) for the 1D model of the top substrate ($\eta=0.1$, $g=10$, and $m=1$).

of the flow of energy into the moving block, which occurs in the one-dimensional model because the density of phonon states at $\omega=0$ is nonzero. This is a peculiarity of the one-dimensional model, but we show in Sec. II D that a minimum in $F(v)$ still exists in a three-dimensional model, so that the results that we derived are qualitatively preserved for a realistic case.

C. One-dimensional semi-infinite substrate: simulation results

Now let us check the analytical results of the previous section with the help of direct simulation of the same model. Let the sliding block consist of N atoms (corresponding to N layers), each having the mass $m=1$. The first layer moves in the external sinusoidal potential due to the bottom substrate, and the dc force F is applied to the last layer of the top substrate, so that the equations of motion are

$$\ddot{x}_1 + \eta\dot{x}_1 + \eta_1(\dot{x}_1 - \dot{x}_2) + g(x_1 - x_2) + \sin x_1 = 0, \quad (29)$$

$$\ddot{x}_l + \eta_l(2\dot{x}_l - \dot{x}_{l-1} - \dot{x}_{l+1}) + g(2x_l - x_{l-1} - x_{l+1}) = 0, \quad l = 2, \ldots, N-1, \quad (30)$$

$$\ddot{x}_N + \eta_N(\dot{x}_N - \dot{x}_{N-1}) + g(x_N - x_{N-1}) - F = 0. \quad (31)$$

To simulate the semi-infinite substrate, the damping η_l inside the moving block was chosen to be zero at the interface and to increase smoothly far away from the interface, as

$$\eta_l = \eta_m \frac{h_l - h_1}{h_N - h_1}, \quad h_l = \tanh\left(\frac{l - L_d}{\Delta L}\right), \quad l = 1, \ldots, N, \quad (32)$$

where we choose $L_d=0.6N$, $\Delta L=N/7$, and $\eta_m=10\omega_s$ (recall that $\omega_s=1$ in our system of units). It is important to notice that the value of η_m is not significant. The role of this damping, which only acts far from the bottom substrate, is to prevent the phonon waves generated in the sliding block at the contact with the substrate from being reflected on the boundary of the moving block and coming back to the contact. Physically, this means that the thickness of the moving block is large enough and that the energy generated at the contact can be dissipated at the top of the block. We emphasize that in the simulation we use a constant-force algorithm, contrary to the constant-velocity assumption used in the analytical approach. However, as we will see from the results, both approaches lead to the same results.

In Fig. 6 we present the simulation results and compare them with those of the analytical Green-function approach of Sec. II B. One can see that the agreement is rather good, realizing that in the analytical approach we took into account only the main harmonic of the force exerted by the substrate and neglected all higher-order ones. These results with a one-dimensional model validate our approximate Green-function approach. Although it is not a strict proof of its validity in higher dimensions, it allows us to use that approach with more confidence in the three-dimensional case, where it becomes the only practical method. Reliable simulations cannot be performed in this case because the one-dimensional

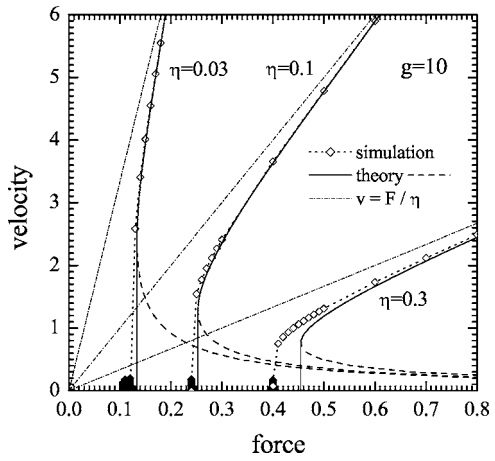

FIG. 6. The dependencies $v(F)$ for the 1D top substrate with $g=10$ for three values of the external damping coefficient $\eta=0.03$, 0.1, and 0.3. The approximate analytical results are shown by solid curves (the unstable branches, by dashed curves), the dash-dotted lines describe the trivial contribution $v=F/m\eta$, and the simulation results, by open diamonds and dotted curves ($N=2048$, $\tau_{\text{wait}}=5\times10^4\tau_0$, $\tau_{\text{measure}}=5\times10^2\tau_0$).

example shows that a very large number of layers ($>10^3$) [as well as a suitable choice of the damping], is required to get results that are not affected by waves reflected on the top surface of the block, and are stable with respect to small parameter changes.

The transition itself is shown in Fig. 7. One can see that the trajectories of atomic layers look similar to the trajectory of the single atom presented in Fig. 1. The inset of Fig. 7 also clearly demonstrates that, when the sliding block stops, the vanishing of the velocity oscillations, excited by the substrate, propagates as a signal in the top substrate, leading to a gradual stopping of the sliding block.

This behavior occurs because the damping η_l given by Eq. (32) is such that it prevents the reflection of the waves sent from the contact into the sliding block. It is interesting

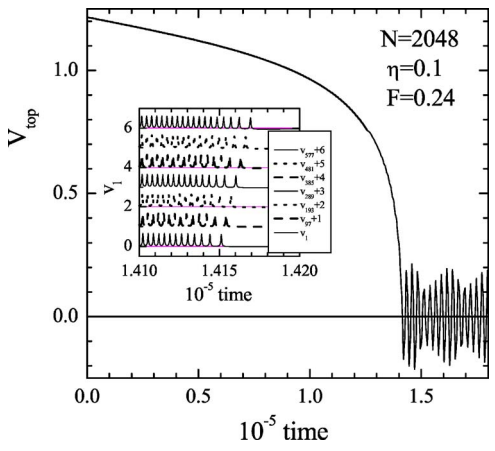

FIG. 7. (Color online) The transition from the smooth sliding to the locked state. The average velocity of the sliding block versus time for a driving force decreased down to $F=0.24$, for 1D sliding block of $N=2048$ atom, with $g=10$ and $\eta=0.1$. Inset: the velocities of some selected layers of the top substrate.

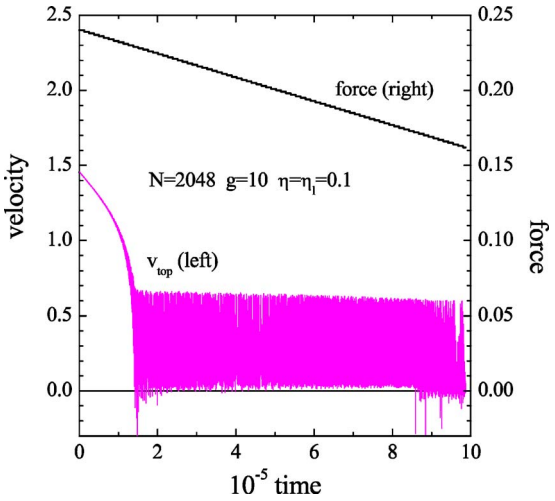

FIG. 8. (Color online) The transition from sliding to the locked state when the force decreases with time for a 1D top substrate of $N=2048$ layers with the constant damping $\eta_l=0.1$ in the substrate ($g=10$, $\eta=0.1$).

to notice that if one chooses η_l to be constant (which could model the situation when the top block corresponds to a thin slab, which could be attached to another large block so that a reflecting interface exists), then the wave generated at the sliding interface and propagating through the substrate is reflected from the top surface of the slab and goes back. A standing wave is excited in the slab, especially for small values of η_l. The energy carried by this wave tends to prevent the transition to the locked state and the sliding state persists now for much smaller values of the dc force, as shown in Fig. 8.

This resonance effect clearly depends on the width of the top block: the narrower the slab, the larger is v_{top}, and the smooth sliding persists for smaller forces, as demonstrated in Fig. 9.

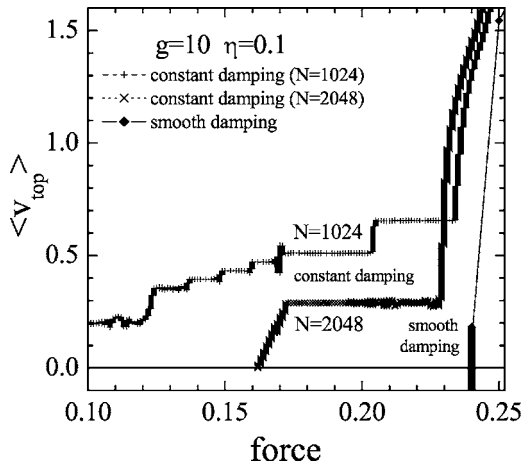

FIG. 9. The averaged velocity of the top substrate as a function of the dc force for the 1D model of the top substrate with a constant damping $\eta_l=0.1$ ($g=10$, $\eta=0.1$, $\tau_{\text{measure}}=2\times10^3\tau_0$). The simulation results from Fig. 6 for the smooth damping given by Eq. (32) are shown for comparison.

D. Three-dimensional substrate

The Green-function technique can be extended to three-dimensional crystals as described in Refs. [21,22]. The lattice Green function is now a six-dimensional matrix. As translational invariance is assumed in the sliding plane, the in-plane components can be expressed in Fourier space, and they depend on a wave vector $\mathbf{k}_\parallel$ in this plane. We shall use an approximate expression obtained by averaging the lattice Green function over the in-plane Brillouin zone, so that, as in the one-dimensional case, it only depends on two spatial indices denoting layers orthogonal to the sliding plane. We henceforth denote $G(\omega)$, as before, the component $G_{11}(\omega)$ of the lattice Green function averaged in the sliding plane. It is the only component of interest here, from which the local density of phonon states $\rho(\omega)=\rho_{11}(\omega)$ can be obtained from Eq. (8). With this approach, for the semi-infinite three-dimensional substrate, the imaginary part of the Green function can be approximated by the expression [22]

$$\begin{aligned}\mathrm{Im}\, G(\omega) &= -\frac{16}{\omega_m^6}\omega(\omega_m^2-\omega^2)^{3/2} \\ &= -\frac{16}{\omega_m^2}\xi(1-\xi^2)^{3/2}, \end{aligned} \tag{33}$$

where $\xi=\omega/\omega_m$, $|\xi|\leqslant 1$. The real part of the Green function can be found numerically with the Kramers-Kronig relation

$$\begin{aligned}\mathrm{Re}\, G(\omega) &= \frac{2}{\pi}\int_0^\infty d\omega_1 \frac{\omega_1}{\omega_1^2-\omega^2}\,\mathrm{Im}\, G(\omega_1) \\ &= \frac{32}{\pi\omega_m^2}\int_0^1 dy \frac{y^2(1-y^2)^{3/2}}{(\omega/\omega_m)^2-y^2}. \end{aligned} \tag{34}$$

The local density of phonon states at the surface is equal to

$$\rho(\omega) = \frac{32}{\pi\omega_m^6}\omega^2(\omega_m^2-\omega^2)^{3/2}. \tag{35}$$

The substitution of this expression into Eq. (9) yields

$$F_1 = \frac{8f_0^2}{m\omega_m^3}\left(\frac{2\pi}{a}\right)^2\left(1-\frac{\omega_0^2}{\omega_m^2}\right)^{3/2}\langle v\rangle. \tag{36}$$

Then, using $|G|^2=(\mathrm{Re}\, G)^2+(\mathrm{Im}\, G)^2$ and taking the integral (34) at $\omega=0$, which gives $\mathrm{Re}\, G(0)=-6/\omega_m^2$, in the limit $\langle v\rangle \to 0$ we obtain

$$|v_0| = \frac{6f_0}{m\omega_m^2}\left(\frac{2\pi}{a}\right)\langle v\rangle \tag{37}$$

and

$$F_3 = \frac{18\eta f_0^2}{m\omega_m^4}\left(\frac{2\pi}{a}\right)^2\langle v\rangle. \tag{38}$$

It is important to point out that, as in our previous analytical calculations, this result has been derived with the assumption that the sliding block is only excited at the washboard frequency ω_0; i.e., all higher-order harmonics have been neglected in the expression of the force exerted by the bottom substrate.

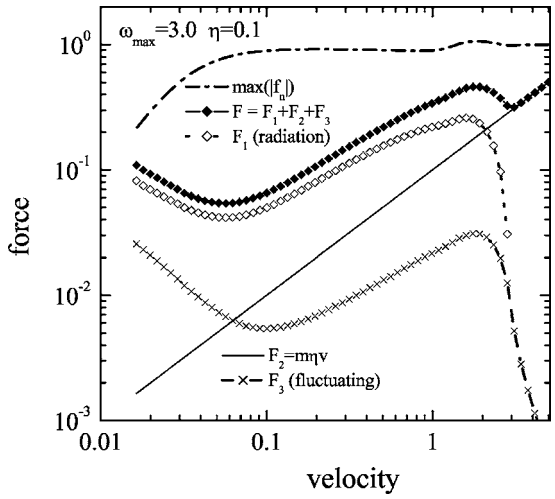

FIG. 10. The dependence $F(v)$ and its contributions for the three-dimensional model of the top substrate.

In this approximation, in the limit $\langle v\rangle \to 0$ we obtain (recall $m=1$ and $f_0=1$) $F_1=(8/\omega_m^3)\langle v\rangle$, $F_2=\eta\langle v\rangle$, and $F_3=(18\eta/\omega_m^4)\langle v\rangle$. Therefore, the friction force is simply proportional to $\langle v\rangle$, so that no locking transition should be expected; i.e., $v_b=0$ and $F_b=0$. This is a sharp contrast with the result obtained with the one-dimensional model of the sliding block, and it appears because, in the limit $\omega\to 0$, the density of phonon states tends to zero for the 3D model of the sliding block, contrary to the 1D model described above. However, at a low velocity of the top block, the motion of the atoms becomes highly anharmonic, similar to the situation described in Sec. I for the single atom, and the higher-order harmonics of the washboard frequency $\omega_0=2\pi\langle v\rangle/a$ must be taken into account. When the velocity is low enough, these high-order harmonics are within the phonon band where the radiation losses are finite. As a result, the contributions F_1 and F_3 are nonzero, and even grow, when $\langle v\rangle \to 0$, as shown in Fig. 10, which has been obtained with the iterative numerical process described in Sec. II A. In Fig. 11 we show the behavior of $F(v)$ for different parameters of the top substrate. One can see that, in all cases, the function $F(v)$ has a minimum at some value $v=v_b>0$. *Thus, the sliding-to-locked transition is discontinuous*.

Therefore, although the analytical calculation restricted to the fundamental frequency of the force exerted by the substrate on the sliding block points out an essential difference between the 1D and 3D models, due to the difference in their phonon density of states around $\omega=0$, the self-consistent calculation, taking into account the higher harmonics that become very important at low velocity, shows that both models give *qualitatively the same result* because there is a rise of F_1 and F_3 at low velocity, which, combined with the variation of F_2 proportional to $\langle v\rangle$, gives in all cases a minimum of the total friction force for some nonzero velocity v_b.

III. SLIDING WITH A LUBRICANT FILM

In the previous section we considered the simple case of "dry" friction, in which a (nonrigid) top block slides over the

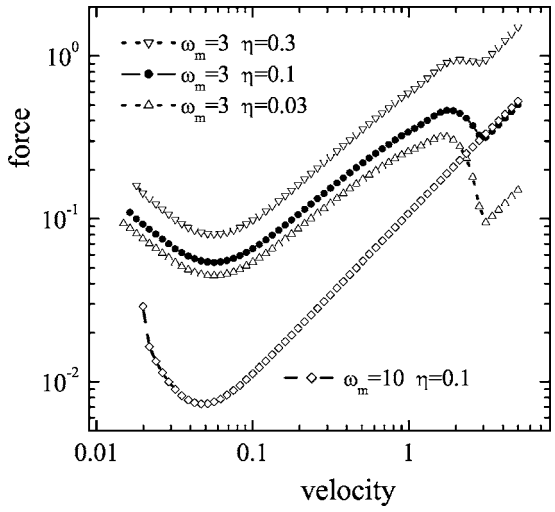

FIG. 11. The dependence $F(v)$ for the 3D model for different model parameters, as shown in the legend.

(rigid) bottom substrate modeled as an external sinusoidal potential. We showed that the velocity v_b at which a running-to-locked transition occurs is not zero, even for an infinite sliding block; therefore, the disagreement between the experimentally observed very low threshold velocity for the stick slip and the velocity observed in simulations cannot be attributed to the small size of the simulated systems. Another explanation for the disagreement could come from the fact that, in experiments, it is practically impossible to realize a true dry friction. Even with perfect surfaces, the unavoidable wear may generate a film of nonsolid material between the sliding block and the substrate. In the present section we show that the result that $v_b \neq 0$ remains unchanged when the sliding block and the bottom substrate are separated by a thin lubricant film. We concentrate our attention on the properties coming from this film. The sliding block is replaced by a dc force applied to the top of the film, which amounts to assuming that the sliding block is fully rigid. The properties of a system with a lubricant film and a deformable sliding block could be deduced from the combination of the results of Sec. II and the present section. However, as we shall show that the lubricant itself does not lead to a vanishing value for v_b, the main result that v_b is finite holds.

A. Layer-over-layer sliding

First, in order to get an analytical insight, we consider a simplified model wherein the top and bottom substrates are kept apart by a lubricant film consisting of N_l *rigid* layers that can slide with respect to each other. Each layer interacts with its two neighbors via a sinusoidal potential, so that the problem is reduced to a one-dimensional lattice with the following equations of motion:

$$m_l\ddot{x}_l + m_l\eta_l(\dot{x}_l - \dot{x}_{l-1}) + m_l\eta_{l+1}(\dot{x}_l - \dot{x}_{l+1}) + \sin(x_l - x_{l-1}) + \sin(x_l - x_{l+1}) = 0, \quad l = 1, \ldots, N_l, \tag{39}$$

where $x_0=0$ corresponds to the bottom substrate and $x_{N_l+1} \equiv x_{\mathrm{top}}$ is the coordinate of the top substrate to which the dc force F is applied;

$$m_{\mathrm{top}}\ddot{x}_{\mathrm{top}} + m_{\mathrm{top}}\eta_{N_l}(\dot{x}_{\mathrm{top}} - \dot{x}_{N_l}) + \sin(x_{\mathrm{top}} - x_{N_l}) = F. \tag{40}$$

For the sake of simplicity we consider only the case of $m_l = m = 1$ and $\eta_l = \eta$ because other values do not qualitatively change the results, and, in particular, the orders of magnitude, which are what we are attempting to determine here, are the same. Equating the energy gain and loss as we did in Eq. (1), we can write

$$F = m\eta\frac{1}{\tilde{a}}\int_0^{\tilde{\tau}} dt \times\left\{(v_{\mathrm{top}} - v_{N_l})v_{\mathrm{top}} + \sum_{l=1}^{N_l}[(v_l - v_{l-1})v_l + (v_l - v_{l+1})v_l]\right\}, \tag{41}$$

where $\tilde{a}=(N_l+1)a$ and $\tilde{\tau}=\tilde{a}/\langle v_{\mathrm{top}}\rangle$. Equation (41) can be rewritten as

$$F = \sum_{l=0}^{N_l}\mathcal{F}[v_{l+1}(t) - v_l(t)], \tag{42}$$

where

$$\mathcal{F}[v(t)] = m\eta\frac{1}{\tilde{a}}\int_0^{\tilde{\tau}} dt v^2(t). \tag{43}$$

Again, the functional (43) can be split into two parts, $\mathcal{F}[v]=(\langle v\rangle/\langle v_{\mathrm{top}}\rangle)\{\mathcal{F}_2[v]+\mathcal{F}_3[v]\}$: the trivial contribution $\mathcal{F}_2[v]=m\eta\langle v\rangle$ and the fluctuating contribution $\mathcal{F}_3[v] = (m\eta/\langle v\rangle\tilde{\tau})\int_0^{\tilde{\tau}}dt[v(t)-\langle v\rangle]^2$.

As an example, let us consider the one-layer lubricant film ($N_l=1$). In the steady state, when the lubricant slides with the velocity v_l over the bottom substrate and with the velocity $v_{\mathrm{top}}-v_l$ with respect to the top substrate, the frictional force $F(v_l)$ applied to the lubricant film from the bottom substrate, should be equal to the force $F(v_{\mathrm{top}}-v_l)$ acting on the lubricant film from the top substrate. A schematic solution of the equation $F(v_l)=F(v_{\mathrm{top}}-v_l)$ is shown in Fig. 12. When the driving velocity is very high, so that $F(v_{\mathrm{top}}) > F_s$, there is only one symmetric solution $v_l=v_{\mathrm{top}}/2$. At lower velocities ($v_{\mathrm{top}} > 2v_b$), there are three solutions, the symmetric one and two asymmetric solutions: $v_l=0$ (the lubricant is attached to the bottom substrate) and $v_l=v_{\mathrm{top}}$ (the lubricant is attached to the top substrate). At low driving velocity ($v_b \leqslant v_{\mathrm{top}} \leqslant 2v_b$), only two asymmetric solutions exist. Finally, at $v_{\mathrm{top}} < v_b$, there are no sliding solutions at all.

These qualitative considerations are confirmed by numerical solutions of Eqs. (39) and (40) presented in Figs. 13 and 14. One can see that the symmetric regime is stable only for a high sliding velocity, when the gradient of the velocity between the nearest layers Δv is large enough (i.e., $\Delta v \gtrsim 2.5$ for the parameters used in Figs. 13 and 14), and the sinusoidal potential is not too dominant. When the driving force decreases, the symmetric sliding becomes unstable, and finally the sliding stops.

The kinetic frictional force in the layer-over-layer sliding regime can be derived from Eqs. (42) and (43), if we approximate the sliding velocities by the first harmonic only,

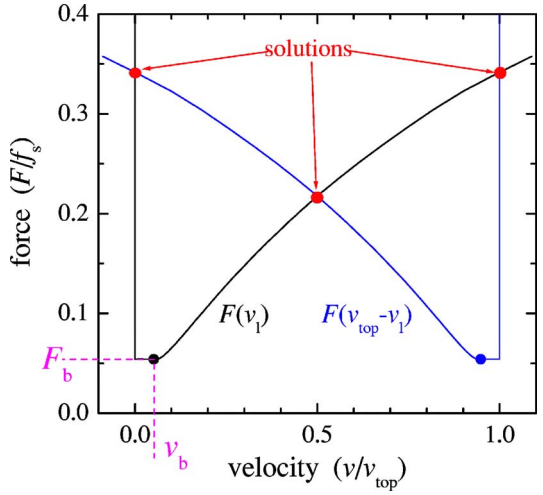

FIG. 12. (Color online) Graphical solution of the equation $F(v_l)=F(v_{top}-v_l)$ for the one-layer lubricant film. The curves $F(v)$ are schematic. The case shown in this figure corresponds to the intermediate velocity range $v_{top}>2v_b$, which has three solutions.

$v_{l+1}(t)-v_l(t)\approx\Delta v_l+v_{fl}\sin(\omega_{fl}t)$, where Δv_l corresponds to the average relative velocity of the adjusted layers, v_{fl} describes the velocity oscillation, and $\omega_{fl}=(2\pi/a)\Delta v_l$. The kinetic friction is then equal to

$$F=\sum_{l=0}^{N_l}\frac{\Delta v_l}{v_{top}}\left(m\eta\Delta v_l+\frac{m\eta}{2\Delta v_l}v_{fl}^2\right). \tag{44}$$

In the symmetric steady-sliding regime, when all layers slide over one another, we have $\Delta v=v_{top}/(N_l+1)$ for all l, and

$$F=\frac{m\eta v_{top}}{N_l+1}\left\{1+\frac{1}{2}\left[\frac{(N_l+1)v_f}{v_{top}}\right]^2\right\}. \tag{45}$$

Otherwise, in the totally asymmetric case, when there is only one sliding interface, we have

$$F\approx m\eta v_{top}. \tag{46}$$

The transition from symmetric to asymmetric sliding with decreasing of the driving velocity was observed by Rozman *et al.* [32] in MD simulation of a one-dimensional atomic chain confined between two sinusoidal potentials. The symmetric and asymmetric layer-over-layer sliding regimes have been observed also in the full three-dimensional MD simulation for a "viscous" three-layer lubricant film [15], where the motion of all lubricant atoms was damped by an artificial external damping coefficient $\eta=0.1\omega_s$. In the next subsections, we describe the simulation results obtained with a more realistic damping mechanism.

B. Three-dimensional simulation: the model

If we want to proceed to a more realistic description of the lubricant film, we must drop the assumption of a rigid layer and a uniform damping coefficient within the lubricant. In this case an analytical study is no longer possible and we must rely on three-dimensional molecular dynamics simulations based on Langevin equations with a realistic damping. Because the model and simulation algorithm was described in detail in a previous paper [16], below we only briefly outline their main features. We study a few atomic-layer film between two parallel top and bottom substrates. Each substrate is made of two layers. One is fully rigid, while the dynamics of the atoms belonging to the layer in contact with the confined lubricant is included in the study. The rigid part of the bottom substrate is fixed, while the rigid layer of the top substrate is mobile in the three directions of space x, y, and z.

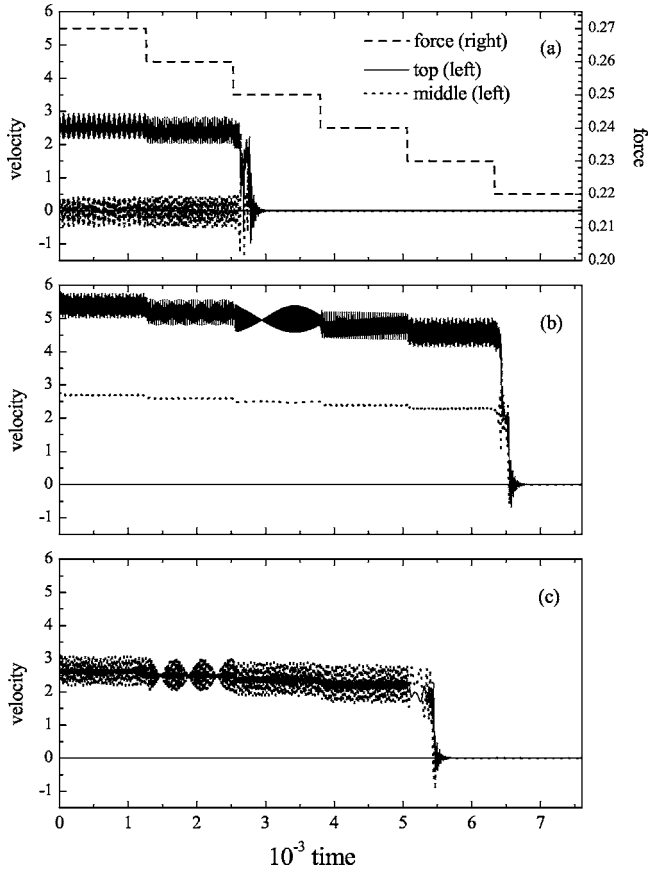

FIG. 13. The velocity of the top substrate and the lubricant layer versus time when the dc force is decreased by small steps (shown by the dashed curve) for the one-layer ($N_l=1$) lubricant film with $m=1$, $\eta=0.1$ for three cases of the initial state: (a) the lubricant is locked to the bottom substrate, (b) the symmetric configuration when the lubricant slides over both the bottom and the top substrates, and (c) the lubricant is locked to the top substrate.

All the atoms interact with Lennard-Jones potentials $V(r)=V_{\alpha\alpha'}[(r_{\alpha\alpha'}/r)^{12}-2(r_{\alpha\alpha'}/r)^6]$ with parameters that depend on the type of interacting atoms. The usual truncation to $r\leqslant r^*=1.49r_{ll}$ is used. Between two substrate atoms we use $V_{ss}=3$ and the equilibrium distance is $r_{ss}=3$. The interaction between the substrate and the lubricant is always much weaker, with $V_{sl}=1/3$. For the lubricant itself, we consider two cases henceforth denoted by "soft lubricant" and "hard lubricant," although, in both cases, the lubricant is always less rigid than the substrates. The soft lubricant uses $V_{ll}=1/9$ and it describes the case of a lubricant made of weakly interacting molecules. The hard lubricant uses V_{ll}

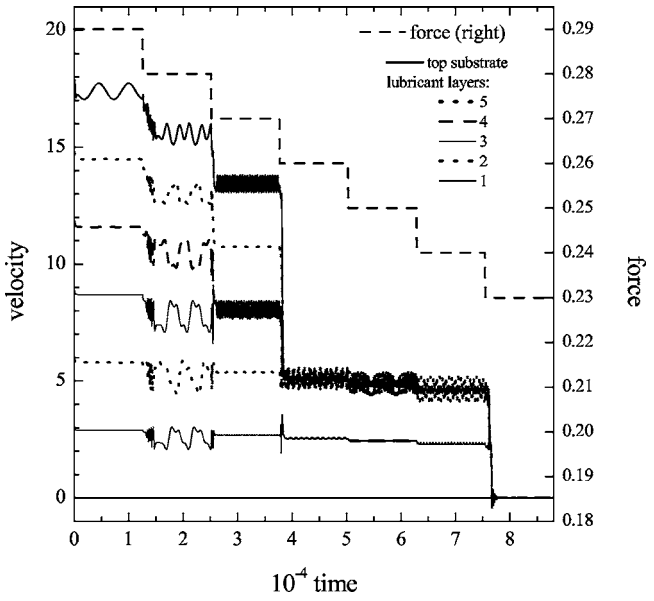

FIG. 14. The same as Fig. 13 for the five-layer lubricant film (N_l=5). The initial state corresponds to the symmetric sliding configuration.

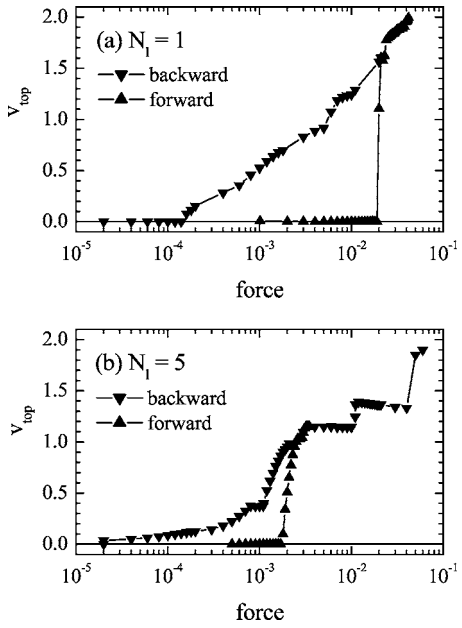

FIG. 15. Hysteresis of the $v_{top}(f)$ dependence for the hard lubricant (V_{ll}=1): (a) one-layer lubricant and (b) five-layer lubricant film.

=1. The equilibrium distance between lubricant atoms is r_{ll} =4.14; i.e., it is "incommensurate" with the equilibrium atomic distance in the substrate. The parameter r_{sl} characterizing the interaction between the substrate and the lubricant is $r_{sl}=\frac{1}{2}(r_{ss}+r_{ll})$. The atomic masses are $m_l=m_s=1$. All the parameters are given in dimensionless units defined in Ref. [16]. The two substrates are pressed together by a loading force that is equal to $f_{\text{load}}=-0.1$ per atom of the top substrate layer.

The main additional feature of our calculations lies in the coupling with the heat bath; i.e., the part of the material that is not explicitly included in the simulation. We use Langevin dynamics with a damping coefficient η that has been designed to mimic a realistic situation, and is presented in detail in Ref. [16]. In a system such as the one that we consider here, the energy loss comes from the degrees of freedom that are not included in the calculation; i.e., the transfer of energy to the bulk of the two substrate materials. Therefore, the damping must depend on the distance z between an atom and the substrate. Moreover, the efficiency of the transfer should depend on the velocity v of the atom because it affects the frequencies of the motions that it excites within the substrates. The damping is written as $\eta(z,v)=\eta_1(z)\eta_2(v)$ with $\eta_1(z)=1-\tanh[(z-z^*)/z^*]$, where z^* is a characteristic distance of the order of the lattice spacing. The expression of $\eta_2(v)$ is deduced from the results known for the damping of an atom adsorbed on a crystal surface. It includes a frequency-dependent phonon term and an additional damping due to the creation of electron-hole pairs in the substrate [16,22,23].

In order to detect the minimal possible sliding velocity such that the motion remains smooth, we used three different algorithms: the constant-force algorithm with adiabatically changed dc force applied to the rigid part of the top substrate, the constant-velocity algorithm when a spring is attached to the top substrate and its free end moves with a constant velocity, and "free runs" when, starting from a sliding state, the force is removed and the system relaxes finally to the locked state. The simulations exhibit the typical behaviors of tribological systems, the hysteresis of the force-velocity dependence and the transition from stick-slip motion to smooth sliding with increasing of the driving velocity. Although the mechanisms of sliding are different for the hard and soft lubricants (the inertia mechanism for the hard lubricant and the melting/freezing mechanism for the soft lubricant), in all cases we found that the critical velocity is of atomic-scale value.

C. The case of a hard lubricant: the inertia mechanism

For the case of the hard lubricant (V_{ll}=1), the lubricant film remains solid during sliding. The typical hysteretic dependencies $v_{top}(f)$ are presented in Fig. 15. When the driving force increases adiabatically (with the constant-force algorithm), the sliding begins at the threshold force $F_s=N_s f_s$, where f_s is the force per atom and N_s is the number of atoms in the rigid layer of the top substrate. Then, if the force decreases starting from the sliding state, a backward transition takes place at $f=f_b<f_s$, and the velocity drops down from a finite value $v_{top}=v_b$ to zero.

The same drop of the velocity is observed in free runs, when one starts with the solid-sliding steady-state regime and the driving force is then removed, so that the top substrate continues to slide due to inertia. The velocity v_{top} slowly decreases until it reaches the minimal value v_b and then drops to zero as shown in Fig. 16 (although in the simulation we typically used m_s=1 for the mass of substrate atoms, the bottom row in Fig. 16 also presents the results for a much higher atomic mass of the substrate).

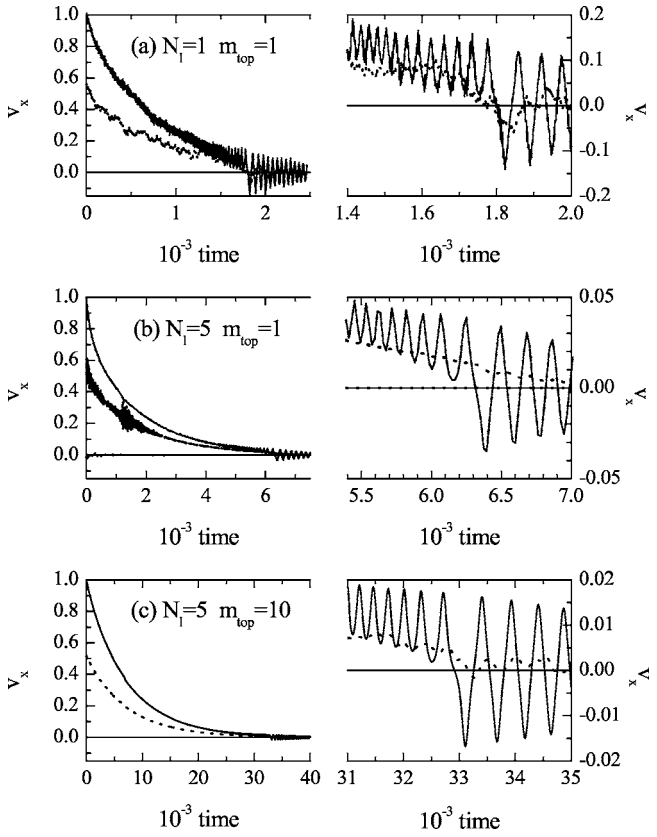

FIG. 16. Free runs starting from the solid-sliding regime for the hard lubricant ($V_{ll}=1$). The velocity of the top substrate (solid curves) and the average velocity of the lubricant (dotted curves) versus time for (a) one-layer lubricant with $m_s=1$, (b) five-layer lubricant film with $m_s=1$, and (c) five-layer lubricant film with $m_s=10$. The right panels demonstrate the scenarios near the sliding-to-locked transition.

The observed hysteresis is well described by the inertia mechanism analogously to the single-particle model described in Sec. I. If the top substrate consisting of two layers is treated as a rigid object, then the critical velocity can be estimated as (for details, see Ref. [16])

$$v_{bR}=\left(\frac{4}{\pi^3}\frac{af_s}{m_s}\right)^{1/2}\approx 0.6\sqrt{f_s}, \tag{47}$$

where we have to take $a=r_{ss}=3$. In the simulation we found that the static frictional force is $f_s\sim 10^{-3}-10^{-2}$, which gives $v_{bR}\sim 0.02-0.06$.

In a large series of runs [16,24], we found that the critical velocity of the transition from stick-slip motion to smooth sliding is $v_c\sim 0.03-0.1$ for the case of "perfect sliding," when the lubricant has an "ideal" crystalline structure incommensurate with the substrate, and $v_c\sim 0.1-0.5$ for the case of an "amorphous" structure of the hard lubricant obtained with the melting/freezing cycles.

D. A soft lubricant: the melting/freezing mechanism

In the case of the soft lubricant ($V_{ll}=1/9$), the scenario is different. Now the lubricant film melts just at the onset of sliding at $F=N_sf_s$. During sliding the lubricant film is strongly heated and remains in the molten state. The effective temperature of the lubricant is approximately linearly proportional to the driving velocity v_{top}. Therefore, when the force and/or velocity decreases, the effective temperature decreases as well, until it becomes lower than the melting temperature of the lubricant film. After that, the lubricant film almost immediately freezes back due to very fast energy exchange with the substrates. The system exhibits hysteresis (see Fig. 17): when the force decreases starting from the sliding state, the backward transition takes place at $f=f_b<f_s$.

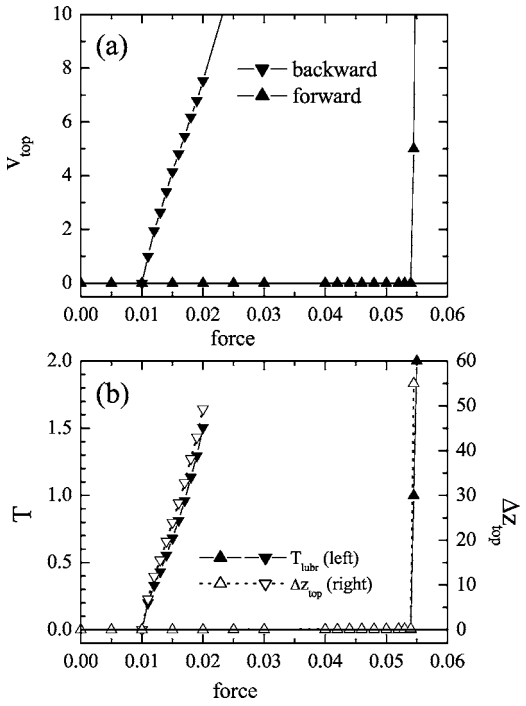

FIG. 17. "Melting-freezing" mechanism of the hysteresis for the soft lubricant ($V_{ll}=1/9$): (a) the $v_{\mathrm{top}}(f)$ dependence and (b) the lubricant temperature (left axes, solid symbols and curves) and the change of the lubricant width (right axes, open symbols and dashed curves) versus force.

However, again the threshold velocity v_b is of atomic-scale value ($v_b\sim 0.1-0.6$), and does not depend on the total mass or size of the top block [16,24].

E. The algorithm with an attached spring

Now let us attach a spring to the top substrate and move its free end with a constant velocity v. As the end moves forward, the spring stretches and the driving force f increases until it reaches the value of the static threshold f_s. At this moment the sliding starts. The lubricant will remain in the solid state in the case of the hard lubricant, and it melts in the soft-lubricant case. Since, due to hysteretic nature of the $v_{\mathrm{top}}(f)$ dependence, the kinetic frictional force in the sliding state can be lower than f_s, the top plate then accelerates to catch up with the spring end and f decreases. If $v>v_c\sim v_b$, the steady sliding regime takes place. However, if $v<v_c$, the

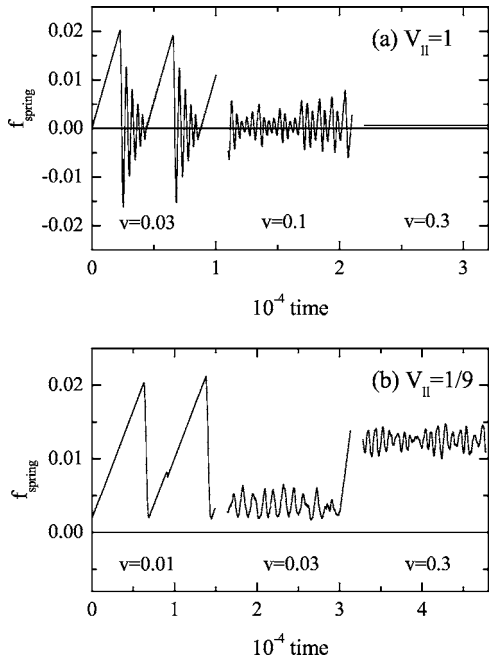

FIG. 18. Spring force versus time when a spring with the elastic constant $k_{\text{spring}}=3\times10^{-4}$ is attached to the top substrate and moves with a constant velocity v. (a) The hard lubricant ($V_{ll}=1$) for velocities $v=0.03$, 0.1, and 0.3; and (b) the soft lubricant ($V_{ll}=1/9$) for velocities $v=0.01$, 0.03, and 0.3.

force decreases down to the lower value f_b, the top plate sticks again, and the process repeats.

Typical dependencies of the spring force versus time are presented in Fig. 18.

In all cases when $f_s\neq0$, the system exhibits a transition from the stick-slip regime at low driving velocity to the smooth sliding at high driving. The transition is typically smooth; the system passes through an intermediate chaotic regime. The details of the transition and the critical velocity v_c may depend on the parameters of the system such as the atomic masses and the elastic constant of the spring, but in all cases v_c remains of atomic-scale order: $v_c\gtrsim0.03-0.5$ [16,24]. In our dimensionless system of units for the chosen set of parameters, the sound speed of the substrate is $v_{\text{sound}}\sim3$ [16]. Thus, if we take a value $v_{\text{sound}}\sim10^3$ m/s for a typical solid, we come to the values $v_c\gtrsim10-10^2$ m/s, which is more than six orders of magnitude higher than those typically claimed in experiments: $v_c\sim10^{-6}$ m/s.

IV. DISCUSSION AND CONCLUSION

Using several approaches different from the analytical one for the semi-infinite three-dimensional substrate to molecular dynamics based on Langevin equations with a realistic coordinate- and velocity-dependent damping, we have shown that the minimally possible velocity when the sliding remains smooth, is of atomic-scale value ($v_b\sim10$ m/s), provided the static frictional force is nonzero. This fact has already been obtained in almost all previous MD simulations (see, e.g., Ref. [5] and references therein). However, there were speculations that this is an artifact of MD simulation because of typically too small sizes of the simulated system, and that in a real situation the critical velocity should scale as $v_b\propto M^{-1/2}$ with the (macroscopic) mass M of the sliding block [5,7]. We have proven that this is not true: the simulation does give correct values of the velocity. Moreover, the critical velocity does not depend on the total mass of the sliding block. Recently, this fact was also confirmed by Luan and Robbins [25] with MD simulations.

The physics of this phenomenon lies in the dynamics of the transition from smooth sliding to the pinned state. When the lowest layer of the sliding block stops, the block does not stop at once. A "stopping wave" is created and propagates into the block, taking away the (macroscopic) kinetic energy of the sliding block. This wave is damped in the block, and the energy is finally transformed into heat. This mechanism was first proposed by Persson [11].

In the present work we have proved the Persson conjecture analytically. The 1D model is solved exactly. For the 3D model, we had to use the averaged Green function to solve the problem, but the phonon spectrum of the semi-infinite substrate is nevertheless introduced correctly so that the approximation can, at most, introduce an error of one order of magnitude, much smaller than the discrepancy between microscopic and macroscopic results that we intend to analyze. Moreover, our approach shows the difficulty of MD simulation of a "macroscopically large" sliding block: If one wants to make realistic simulations, the block height H should be larger than 10^3 atomic layers, and special attention should be given to the damping of elastic waves in the block. Otherwise, due to interference of the stopping wave with the wave reflected by the opposite surface of the block, a standing wave is created, and it perturbs the sliding-to-locked transition. In this case the critical velocity v_b scales with the height of the sliding block as $v_b\propto H^{-1/2}$, as was recently observed by Luan and Robbins [25] in MD simulation, where a constant artificial damping was used. Because $M\propto H$, such simulations lead to a (physically wrong) conclusion that $v_b\propto M^{-1/2}$.

The minimally possible velocity v_b determines in turn the critical velocity v_c of the transition from stick-slip motion to smooth sliding: $v_c\sim v_b$. Thus, the simulations as well as the analytical approach predict that the transition to smooth sliding should take place at a huge velocity $v_c\sim10$ m/s. This is in strong disagreement with macroscopic experiments, where a transition to smooth sliding is typically observed at $v_c\sim1$ μm/s [2–4]. However, precise experiments show that stick-slip regime in fact persists at all velocities experimentally available (see, e.g., the experimental results by Klein and Kumacheva [26] and by Budakian and Putterman [28]).

Another fact directly connected with this question concerns the effective viscosity $\tilde{\eta}$ of a thin lubricant film, which is determined by a relationship $\tilde{\eta}\propto f_k/v_c$. Using experimental values $v_c\sim1$ μm/s leads to a common conclusion that the viscosity of a thin lubricant film is many orders of magnitude larger than that of the bulk lubricant, while MD simulation predicts that the viscosity of the film in the smooth sliding regime should be of the same order as the bulk value. In this context we would like to mention a recent experimental result by Becker and Mugele [29], where dynamics of squeezing of a thin OMCTS film was studied, and the authors came

to the conclusion that mutual friction between adjacent lubricant layers is close to the bulk viscosity.

On the other hand, experimentally observed values of $v_c \sim 1$ μm/s can be explained with the help of the earthquake-like model (see, e.g., Ref. [30] and references therein). These theories assume that the sliding interface consists of many point-like junctions (asperities, contacts, etc.). The models predict that the experimentally observed "smooth" sliding corresponds actually to atomic-scale stick-slip motion of many junctions, while the macroscopic-scale stick-slip behavior appears due to concerted motion of the many junctions due to their elastic interaction. The necessary ingredient of earthquake-like models is the assumption that the static frictional force f_s increases with the time of stationary contact with a characteristic "aging" time τ. The transition should then be observed at $v_c \sim \tilde{a}/\tau$, where $\tilde{a}$ is an average distance between the junctions. Note that if one takes an *exponential* increase of $f_s(t)$ from a lower value f_{s1} to a higher value f_{s2}, then the earthquake-like model predicts three regimes with two (smooth) transitions between them, the smooth sliding with $f_k \sim f_{s2}$ at very low velocities, the smooth sliding with $f_k \sim f_{s1}$ at high velocities, and the stick-slip behavior at intermediate velocities (for details see Ref. [30]). It is interesting that the two transitions indeed were observed experimentally by Drummond *et al.* [31] for sliding of adhesive surfactant-bearing surfaces in water.

The nature of the asperities in earthquake-like models is more or less clear for the contact of two rough surfaces, but it is questionable in the case of contact of two atomically smooth mica surfaces [4]. A discussion on this topic may be found, e.g., in the monograph by Persson [1] and in Ref. [9]. An explanation could also be that there are some defects or impurities in the contact area (see, e.g., Mukhopadhyay *et al.* [27]). Another important question is a mechanism of the $f_s(t)$ dependence, which gives macroscopic aging times $\tau \gtrsim 1$ s. The only such mechanism could be a plastic deformation of a softer part of the contact; i.e., the lubricant film. In the case of lubricants consisting of "simple" molecules an increase of f_s with time may be due to a slow squeezing of the lubricant from the contact area; for the case of long-chain organic lubricants a slow process may be connected with interdiffusion of lubricant molecules [1].

Finally, it is important to note that all results of the present work correspond to a tribological system with a planar geometry, when the area A of the contact scales with a characteristic linear size R of the sliding block as $A \propto R^2$. However, our conclusions cannot be applied to STM-like devices, where a tip of a macroscopic size (e.g., $\sim$1 mm) moves over a surface, because in this case the real contact area consists of only one or a few atoms. In the latter case the total mass of the tip should certainly be important, and v_c would depend on M, as predicted by the MD simulation by Luan and Robbins [25].

ACKNOWLEDGMENTS

We wish to express our gratitude to A. R. Bishop, B. N. J. Persson, J. Röder, and M. Urbakh for helpful discussions. This research was supported in part by the NATO Collaborative Linkage Grant No. PST.CGL.980044. A.V. was partially supported by PRRIITT (Regione Emilia Romagna), Net-Lab "Surface & Coatings for Advanced Mechanics and Nanomechanics" (SUP&RMAN), and by MIUR Cofin 2004023199.

[1] B. N. J. Persson, *Sliding Friction: Physical Principles and Applications* (Springer-Verlag, Berlin, 1998); Surf. Sci. Rep. **33**, 83 (1999).

[2] C. M. Mate, In: *Handbook of Micro/Nano Tribology*, edited by B. Bhushan (CRC Press, Boca Raton, FL, 1995) p. 167.

[3] *Fundamentals of Friction: Macroscopic and Microscopic Processes*, edited by I. L. Singer and H. M. Pollock (Kluwer, Dordrecht, 1992); *Physics of Sliding Friction*, edited by B. N. J. Persson (Kluwer, Dordrecht, 1996).

[4] H. Yoshizawa, Y. L. Chen, and J. Israelachvili, Wear **168**, 161 (1993); H. Yoshizawa and J. Israelachvili, J. Phys. Chem. **97**, 11 300 (1993); G. Reiter, A. L. Demirel, and S. Granick, Science **263**, 1741 (1994); B. Brushan, J. N. Israelachvili, and U. Landman, Nature (London) **374**, 607 (1995); A. D. Berman, W. A. Ducker, and J. N. Israelachvili, Langmuir **12**, 4559 (1996).

[5] M. O. Robbins, in *Jamming and Rheology: Constrained Dynamics on Microscopic and Macroscopic Scales*, edited by A. J. Liu and S. R. Nagel (Taylor and Francis, London, 2000); M. O. Robbins and M. H. Müser, *Computer Simulation of Friction, Lubrication and Wear*, in: *Handbook of Modern Tribology*, edited by B. Bhushan (CRC Press, Boca Raton, FL, 2000).

[6] J. Gao, W. D. Luedtke, and U. Landman, J. Phys. Chem. B **101**, 4013 (1997); J. Phys. Chem. **106**, 4309 (1997).

[7] M. O. Robbins and P. A. Thompson, Science **253**, 916 (1991); P. A. Thompson, M. O. Robbins, and G. S. Grest, Isr. J. Chem. **35**, 93 (1995); A. Baljon and M. O. Robbins, MRS Bull. **22**, 22 (1997).

[8] J. E. Hammerberg, B. L. Holian, J. Röder, A. R. Bishop, and S. J. Zhou, Physica D **123**, 330 (1998); R. P. Mikulla, J. E. Hammerberg, P. S. Lomdahl, and B. L. Holian, Mater. Res. Soc. Symp. Proc. **522**, 385 (1998).

[9] B. N. J. Persson, Phys. Rev. Lett. **71**, 1212 (1993); Phys. Rev. B **48**, 18140 (1993); J. Chem. Phys. **103**, 3849 (1995); Phys. Rev. B **51**, 13568 (1995).

[10] O. M. Braun, T. Dauxois, M. Paliy, and M. Peyrard, Phys. Rev. Lett. **78**, 1295 (1997); Phys. Rev. E **55**, 3598 (1997); M. Paliy, O. Braun, T. Dauxois, and B. Hu, *ibid.* **56**, 4025 (1997).

[11] B. N. J. Persson, Phys. Rev. B **50**, 4771 (1994).

[12] M. Weiss and F.-J. Elmer, Phys. Rev. B **53**, 7539 (1996); Z. Phys. B: Condens. Matter **104**, 55 (1997); O. M. Braun, A. R. Bishop, and J. Röder, Phys. Rev. Lett. **79**, 3692 (1997); O. M. Braun, B. Hu, A. Filippov, and A. Zeltser, Phys. Rev. E **58**, 1311 (1998).

[13] M. G. Rozman, M. Urbakh, and J. Klafter, Europhys. Lett. **39**,

183 (1997); Phys. Rev. Lett. **77**, 683 (1996); Phys. Rev. E **54**, 6485 (1996).
[14] O. M. Braun, T. Dauxois, and M. Peyrard, Phys. Rev. B **56**, 4987 (1997).
[15] O. M. Braun, A. R. Bishop, and J. Röder, Phys. Rev. Lett. **82**, 3097 (1999).
[16] O. M. Braun and M. Peyrard, Phys. Rev. E **63**, 046110 (2001).
[17] H. Risken, *The Fokker-Planck Equation* (Springer, Berlin, 1984), Chap. 11; K. Voigtlaender and H. Risken, J. Stat. Phys. **40**, 397 (1985); H. Risken and K. Voigtlaender, *ibid.* **41**, 825 (1985).
[18] G. Costantini and F. Marchesoni, Europhys. Lett. **48**, 491 (1999); M. Borromeo and F. Marchesoni, Phys. Rev. Lett. **84**, 203 (2000).
[19] O. M. Braun and Yu. S. Kivshar, *The Frenkel-Kontorova Model: Concepts, Methods, and Applications* (Springer-Verlag, Berlin, 2004).
[20] L. D. Landau and E. M. Lifshitz, *Statistical Physics* (Pergamon, London, 1958).
[21] A. M. Kosevich, *Theory of Crystal Lattice* (Vuscha Schkola, Kharkov, 1988).
[22] O. M. Braun, Surf. Sci. **213**, 336 (1989); O. M. Braun and A. I. Volokitin, Fiz. Tverd. Tela (Leningrad) **28**, 1008 (1986) [Sov. Phys. Solid State **28**, 564 (1986)].
[23] O. M. Braun, A. I. Volokitin, and V. P. Zhdanov, Usp. Fiz. Nauk **158**, 421 (1989) [Sov. Phys. Usp. **32**, 605 (1989)].
[24] O. M. Braun (unpublished).
[25] B. Luan and M. O. Robbins, Phys. Rev. Lett. **93**, 036105 (2004).
[26] J. Klein and E. Kumacheva, Science **269**, 816 (1995); J. Chem. Phys. **108**, 6996 (1998); E. Kumacheva and J. Klein, *ibid.* **108**, 7010 (1998).
[27] A. Mukhopadhyay, J. Zhao, S. C. Bae, and S. Granick, Phys. Rev. Lett. **89**, 136103 (2002).
[28] R. Budakian and S. J. Putterman, Phys. Rev. Lett. **85**, 1000 (2000).
[29] T. Becker and F. Mugele, Phys. Rev. Lett. **91**, 166104 (2003).
[30] O. M. Braun and J. Röder, Phys. Rev. Lett. **88**, 096102 (2002).
[31] C. Drummond, J. Israelachvili, and P. Richetti, Phys. Rev. E **67**, 066110 (2003).
[32] M. G. Rozman, M. Urbakh, and J. Klafter, Physica A **249**, 184 (1998); M. G. Rozman, M. Urbakh, J. Klafter, and F.-J. Elmer, J. Phys. Chem. B **102**, 7924 (1998).